Physicochem. Probl. Miner. Process., 57(1), 2021, 75-86

http://www.journalssystem.com/ppmp

Physicochemical Problems of Mineral Processing

ISSN 1643-1049

Received June 29, 2020; reviewed; accepted October 21, 2020

Effect of direct reduction time of vanadium titanomagnetite concentrate on the preparation and photocatalytic performance of calcium titanate

Xiaohui Li, Jue Kou, Tichang Sun, Shichao Wu, Yuechao Tian

University of Science and Technology Beijing

Corresponding author: koujue@ustb.edu.cn (J. Kou)

Abstract: Effects of direct reduction time of vanadium titanomagnetite concentrate (VTCE) on the preparation and photocatalytic performance of calcium titanate were investigated in this study. It was found that extending the reduction time could not only promote the formation of calcium titanate, but also facilitate the reduction of iron minerals in the reduction products. The optimum reduction time was 180min under the conditions of $CaCO_3$ dosage of 18wt%, reduction temperature of 1400℃ and lignite dosage of 70wt%. The reduced iron (Fe grade of 90.95wt%, Fe recovery of 92.21wt%) and calcium titanate were obtained via grinding-magnetic separation. Moreover, calcium titanate prepared via the direct reduction method could be used as a photocatalyst, where the degradation degree of methylene blue increased from 25.13% to 60.14% with the addition of calcium titanate. Furthermore, Langmuir Hinshelwood fitting results indicated that the degradation of methylene blue by the calcium titanate prepared under different reduction times conformed to first-order reaction kinetics, where the photocatalytic degradation rate of methylene blue was noted to be the highest for a reduction time of 180 min.

***Keywords*:** vanadium titanomagnetite concentrate, calcium titanate, direction reduction, metallic iron, photocatalytic performance

1. Introduction

Increasing attention is being paid to the degradation of pollutants by photocatalysts, which has become a new method for solving environmental pollution problems (Singh and Borthakur, 2018; Ani et al., 2018). Perovskite-type photocatalyst is widely used in producing hydrogen by photocatalytic decomposition of water (Alsayegh et al., 2019; Sreethawong et al., 2009), degrading of organic dyes (Xiao et al., 2008), and producing organic substances by photocatalytic reduction of CO_2 (Yue et al., 2019; Pan et al., 2007) since its unique structures. As a typical perovskite structure, calcium titanate has a wide application prospect in the fields of photoelectric sensing, catalysis, dielectric and optics, etc. (Li et al., 2011; Deng, et al., 2020). The conventional methods for synthesizing calcium titanate mainly include solid phase reaction, mechanical synthesis, the sol-gel process, and hydrothermal synthesis (Deng et al., 2020; Lei et al., 2017; Zhang et al., 2012). Among them, the solid-state synthesis method has been widely used in industrial production owing to its advantages of a high yield, a simple process, and mature technology. Through this method, the calcium titanate can be prepared via a conventional solid-state reaction between TiO_2 and $CaCO_3$ or CaO at a temperature of approximately 1400-1600℃ (Zhao et al., 2013; Palaniandy and Jamil, 2009). However, the particle sizes of the calcium titanate powder prepared via this method vary widely, which is not conducive to applications. Additionally, the method requires a high TiO_2 purity (Li et al., 2011). Hence, it is necessary to develop an environment-friendly and low-cost alternative for the preparation of calcium titanate.

Vanadium titanomagnetite is an associated and coexisting mineral, that has a high comprehensive utilization value because it contains various useful elements such as Fe, Ti, and V (Pan et al., 2017; Imtiaz

DOI: 10.37190/ppmp/128684

et al., 2015; Li et al., 2019;). Vanadium titanomagnetite in Panxi Sichuan is a significant source of Fe and Ti in China (Li et al., 2019). However, because of the high contents of Fe and Ti in the vanadium titanomagnetite in Panxi, the traditional grinding method leads to approximately 53% of the Ti entering into the Fe concentrate, and forms blast furnace slag containing 20%-25% Ti after blast furnace ironmaking (Mao et al., 2013; Zhang et al., 2018). Numerous studies have focused on the process of "acid (Li et al., 2016), alkali (Sun et al., 2015), high-temperature carbonization and low-temperature chlorination (Yang et al., 2000)" to recycle titanium resources, but the utilization level of titanium resources in Panxi remains lower. Direct reduction has become one of important processes for Fe-making and Ti-recycling owing to certain advantages of simple operation, relatively short process and low energy consumption (Zhang et al., 2017; Yu et al., 2015). Fe was preferentially reduced to metallic iron, while Ti still existed in the form of oxides during the direct reduction process, which was conducive to separating them via magnetic separation. Ti slag with a TiO_2 content of exceeding 40% could be obtained after magnetic separation. Unfortunately, this Ti-slag is still not a raw material qualified for use in the production of Ti-dioxide, because of its high impurity contents (Chen et al., 2014; Man et al., 2014; Zhao et al., 2019; Yi et al., 2013). Thus, there are still many problems in separating iron and titanium slag via the direct reduction process.

Recent studies (Chen et al., 2017; Li et al., 2020a; Li et al., 2020b) revealed that mixing VTCE with magnesium or calcium compound can reduce iron to metallic iron and transform titanium into magnesium titanate or calcium titanate through the direct reduction of VTCE. If the preparation of magnesium titanate or calcium titanate can be achieved while recovering iron via the reduction of VTCE, this will not only shorten the preparation process of such titanium-containing nonmetal materials, but also provide a new method for the efficient utilization of titanium resources in the Panxi area. However, while ensuring the reduction effect of iron minerals, the foregoing studies focused only on the effects of the calcium compounds, reduction temperature and reductant types on the formation of calcium titanate. The properties and applications of calcium titanate prepared during the direct reduction of VTCE were not investigated. So this paper aims to further optimize the reduction conditions and determine whether this calcium titanate can be used as a photocatalys, and the effect of direct reduction time of VTCE on the preparation and photocatalytic performance of calcium titanate were also investigated.

2. Experimental

2.1. Materials

The vanadium titanomagnetite used in the test was obtained from Panxi, China, and was subjected to low-intensity magnetic separation to obtain VTCE. The results of chemical analysis are presented in Table 1, indicating that the TFe and TiO_2 contents are 56.80wt% and 12.75wt%, respectively. Fig. 1 shows the X-ray diffraction (XRD, Rigaku D/Max 2500, Japan) pattern of VTCE, where Fe exists in the form of magnetite (Fe_3O_4), Ti is mainly present in the form of ilmenite ($FeTiO_3$).

The analytically pure $CaCO_3$ and methylene blue used in this study were sourced from Sinopharm Chemical Reagent Co Ltd, China, where the colour index of methylene blue is C. I. 52015.

The reductant used in this study was lignite with a particle size of less than 1 mm, in which the contents of fixed carbon, ash, volatile matter and moisture were 42.39wt%, 9.46wt%, 32.43wt% and 15.72wt%, respectively.

Table 1. Chemical compositions of the VTCE

Component	TFe	TiO_2	CaO	MgO	Al_2O_3	SiO_2	V_2O_5	MnO
Content / wt%	56.80	12.75	0.57	2.44	3.6	2.21	0.56	0.32

2.2. Methods

The experiment methods mainly include mixing and pelletizing, reduction roasting and grinding-magnetic separation, where the specific experiment process is shown as Fig. 2.

Mixing and pelletizing: 100g of VTCE was mixed with 18wt% $CaCO_3$, and pellets with diameters

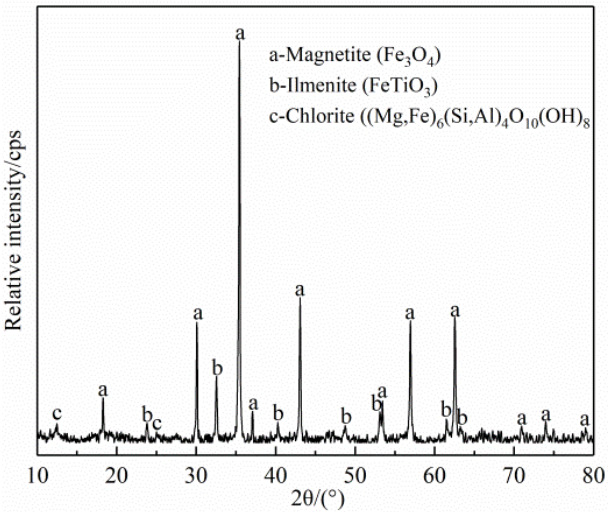

Fig. 1. XRD patterns of VTCE

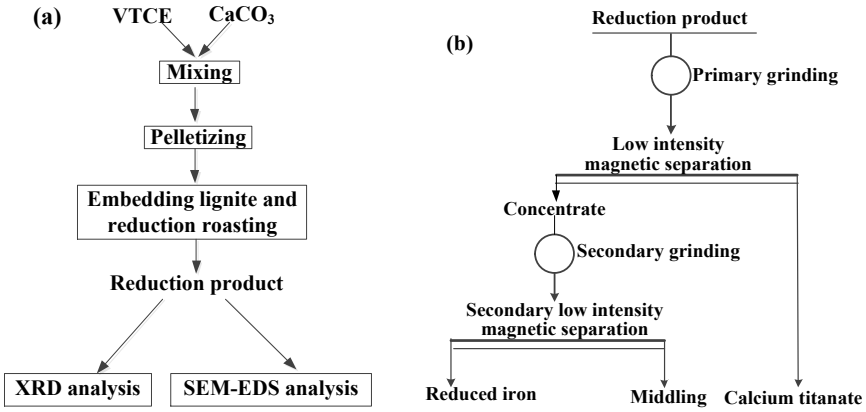

(a)-Reduction and roasting flow sheet; (b)-Grinding-magnetic separation flow sheet

Fig. 2. Reduction roasting and grinding-magnetic separation flow sheet

of approximately 10mm were produced by adding water. The pellets were dried at 100℃ for 5h to obtain green pellets.

Reduction roasting: First, 70wt% lignite together with three green pellets were placed in a graphite crucible with a diameter of 50 mm and height of 70 mm. The green pellets were completely embedded in the lignite to ensure enough reduction atmosphere. The purpose of using embedding method was to prevent the ash in lignite entering the calcium titanate product. The graphite crucible was removed from the furnace. After heating and maintaining for a certain time at 1400℃, the graphite crucible was taken out from the furnace when the temperature had decreased to 60℃, and the reduction products were obtained after the graphite crucible was cooled to room temperature in air.

2.3. Analytical techniques

The analytical techniques used in this study included metallization degree analysis, XRD and scanning electron microscope energy dispersive spectrometer (SEM-EDS) analyses and photocatalytic performance analysis.

2.3.1. Metallization degree analysis

The metallization degree of the reduction product was calculated using Eq. (1), in which, ω_{TFe} is the weight percent of total iron (TFe) in the reduction product, wt%; and ω_{MFe} is that of metallic iron (MFe) in the reduction product, wt%.

$$D_m = \omega_{MF_e}/\omega_{TF_e} \times 100\% \quad (1)$$

2.3.2. XRD and SEM-EDS analyses

A roast pellet was cut along the center line; one half of it was ground to -0.074mm of 80wt% to analyze the changes of mineral composition by XRD (Rigaku D/Max 2500, Japan). The other half was used to analyze the changes of microstructural and the distribution of Fe and Ti by SEM-EDS (CAMBRIDGES-360, VO18, Carl Zeiss, Germany).

2.3.3. Photocatalytic analysis

Photocatalytic degradation of methylene blue as the target of calcium titanate was performed in a photochemical reactor. A Hg lamp with a dominant wavelength of 365 nm and an ultraviolet light intensity of 300W was set in the reactor. The Hg lamp was separated from the reaction liquid via a quartz tube with cooling water circulation to maintain a temperature at about 25℃. Then, 3g/L calcium titanate was added to 100mL of a methylene blue solution at a concentration of 10mg/L, the magnetic stirrer was used to keep catalyst in suspension. It should be noted that the optimum dosage of calcium titanate was 3g/L according to the previous test results of photocatalytic conditions, so in order to ensure the uniqueness of the test variables, the calcium titanate dosage was still set as 3g/L in this study. Before the photocatalytic reaction, the reaction solution was stirred for 30min in the dark to ensure the reaction solution attained adsorption/desorption equilibrium. After the photocatalytic reaction, 10mL of the supernatant was centrifuged every 0.5h to measure the absorbance by UV-Vis spectrophotometer (UV-2800(A)), where the λmax for the concentration of methylene blue was 664nm. The absorbance value was converted to the concentration according to the standard curve, and the degradation degree of methylene blue was calculated using Ep. (2) to evaluate the photocatalytic activity of the calcium titanate.

$$\eta = (a_0 - a_t)/a_0 \times 100\% \quad (2)$$

where η is the degradation degree; a_0 is the methylene blue concentration after reaching adsorption equilibrium, which as the initial concentration of photocatalytic reaction; a_t is the methylene blue concentration at time *t*.

2.3.4. Kinetic analysis of photocatalytic reaction

According to the Langmuir Hinshelwood (LH) model, first-order reaction fitting was performed for the photocatalytic degradation of methylene blue by calcium titanate at different reduction times. The effect of the reduction time of VTCE on the kinetics of photocatalytic degradation of the methylene blue by calcium titanate was calculated.

3. Results and discussion

3.1. Effect of reduction time on calcium titanate formation in direct reduction of VTCE

3.1.1 Effect of reduction time on phase composition of reduction products

A previous study (Li et al., 2019a) revealed that the addition of 18wt% $CaCO_3$ to the direct reduction of VTCE can synchronously form calcium titanate while recovering iron. To further optimize the reduction conditions and determine the optimal reduction time, an XRD analysis was performed on the reduction products at various reduction times, and the results are shown in Fig. 3.

As shown in Fig. 3, the reduction time significantly affected the phase compositions of the reduction products. When the reduction time was 60min, Fe of reduction products was mainly present in the form of metallic Fe and ilmenite ($FeTiO_3$). The Ti mainly existed in ilmenite and calcium titanate ($CaTiO_3$). According to the XRD analysis of the VTCE in the materials, most of the Fe in the VTCE existed in the form of magnetite (Fe_3O_4), and a small amount existed as ilmenite ($FeTiO_3$), Ti in VTCE existed mainly in the form of ilmenite ($FeTiO_3$). The results indicated that magnetite was completely reduced to metallic Fe at 60min, while only a small amount of ilmenite in the reduction product reacted with $CaCO_3$ and formed calcium titanate; most of the Ti still existed in the form of ilmenite. When the reduction time was extended to 90min, the diffraction peaks of ilmenite in the reduction product disappeared, indicating that extending the reduction time was beneficial for the formation of calcium titanate. Beca-

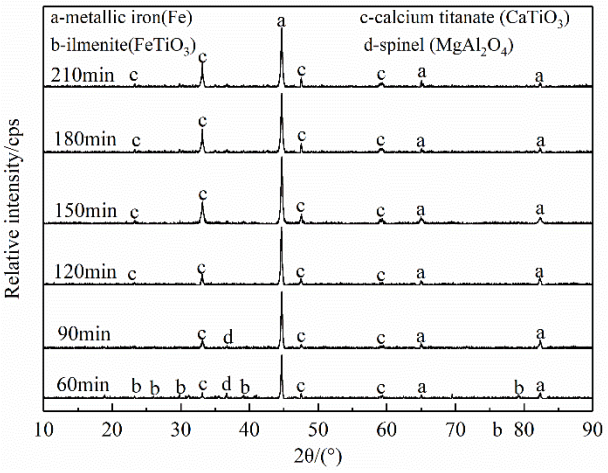

Fig. 3. Effect of reduction time on phase compositions of reduction products

use of the diffraction peaks intensity of calcium titanate in the reduction product was still weaker, the reduction time should be continued extension. When the reduction time was higher than 90min, the phase compositions of the reduction product no longer changed, Fe and Ti were mainly present in the form of metallic Fe and calcium titanate, respectively. Meanwhile, their diffraction peak intensities gradually strengthened with the extension of the reduction time, and better formation was achieved at 180min. However, a further increase in the reduction time had little effect on the formation of calcium titanate.

3.1.2. Effect of reduction time on metallization degree of reduction products

To ensure the comprehensive utilization of Ti and Fe resources in VTCE, the beneficial effect of iron reduction should also be ensured during the investigation of the effect of the reduction time on the preparation of calcium titanate in the reduction of VTCE with the addition of $CaCO_3$. Thus, a chemical analysis was performed on the reduction products at different reduction times. The result is shown in Fig. 4.

As shown in Fig. 4, the metallization degree of the reduction product increased with the reduction time. When the reduction time increased from 60 to 180min, the metallization degree of the reduction products increased from 85.45wt% to 91.90wt%, 94.36wt%, 95.84wt% and 96.20wt%. Clearly, extending the reduction time was conducive to increasing the metallization degree of the reduction product. And these results indicate that the formation of calcium titanate has no adverse effect on the reduction of iron minerals in VTCE. Although the metallization degree of the reduction product increased from 96.20wt% to 96.33wt% when the reduction time was extended to 210min, it changed little change between 180min and 210min. The results indicate that the reduction effect of iron in reduction product was better when the reduction time was 180min, and that the effect of extending the reduction time on the metallization degree was not significant. This phenomenon was consistent with the XRD results.

3.1.3. Effect of reduction time on microstructure of reduction products

Considering the calcium titanate formation and the reduction product metallization degree, the optimum reduction time was 180min. For an in-depth investigation of the generation and purity of calcium titanate and metallic iron particles, SEM-EDS analysis was performed on the reduction product with a condition of $CaCO_3$ dosage of 18wt%, a reduction temperature of 1400℃ and a reduction time of 150min to 210min. The results were shown in Fig. 5.

Fig. 5 performed the SEM-EDS results for the reduction products at different reduction time. According to the elements contents in Fig. 5(d), the lower brightness particles in the reduction products were of calcium titanate with a uniform distribution, and the particle size was approximately 50μm. The reduction time significantly affected the particle size of the calcium titanate. The calcium titanate particle size in the reduction product increased from less than 10μm to more than 20μm when the reduction time increased from 150 to 180min, indicating that the extension of the reduction time was

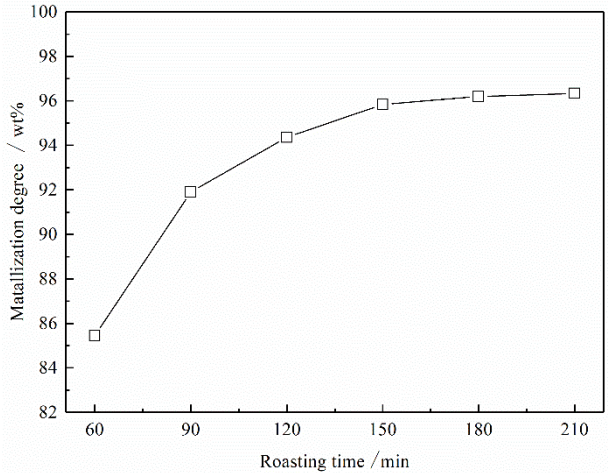

Fig. 4. Effect of reduction time on metallization degree of reduction products

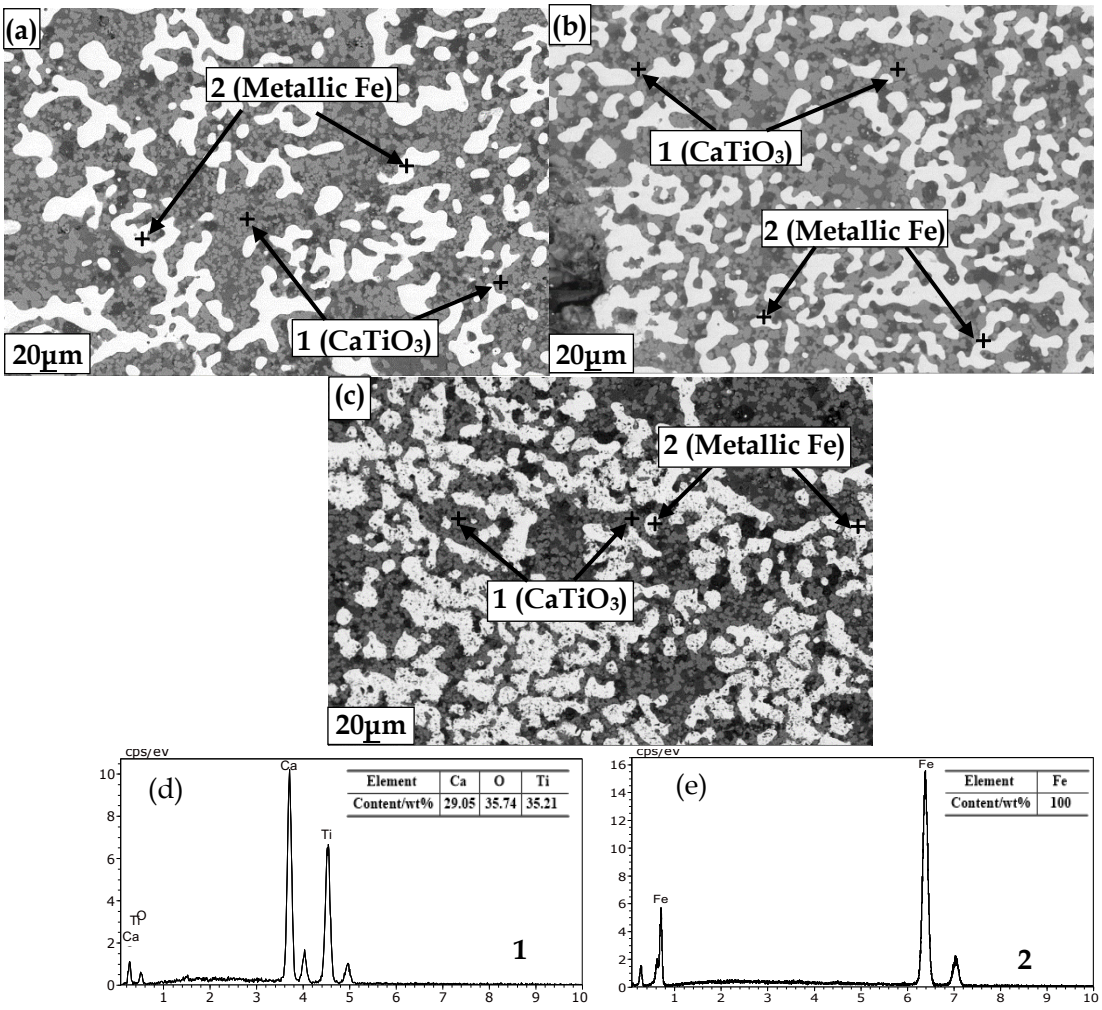

(a), (b), (c)-SEM images of reduction product at 150min, 180min and 210min; (d), (e)-EDS spectra of point 1 and 2

Fig. 5. SEM-EDS analysis of reduction product under optimum roasting time

conducive to the growth of calcium titanate particles and the subsequent separation of calcium titanate and metallic iron through grinding magnetic separation.

Similarly, according to the elements contents in Fig. 5(e), the brightest particles in the reduction products were metallic iron. Clearly, the particle size of the metallic iron particles in the reduction

product was above 50μm at different reduction time, which indicated that the extension of the reduction time had little influence on the metallic iron particle size in the reduction product. However, there were fine-grained materials distributed in the metallic iron particles in the reduction product when the reduction time was 210min, which was not conducive to the subsequent recovery of iron. Therefore, considering the calcium titanate and metallic iron formation, the optimal reduction time was 180 min. Additionally, as indicated by the energy spectrum in Figs. 5(d) and 5(e), there were no impurity elements other than the constituent elements in the metallic iron and calcium titanate particles in the reduction products, suggesting that the purity of the calcium titanate and metallic iron particles was higher at 180min.

In summary, extending the reduction time can not only promote the formation of calcium titanate, but also facilitates the reduction of iron minerals in the reduction products. The optimum reduction time was 180min under the conditions of $CaCO_3$ dosage of 18wt%, reduction temperature of 1400℃ and lignite dosage of 70wt%. Where a better generation effect was achieved for both the calcium titanate and metallic iron could be achieved.

3.2. Effect of reduction time on photocatalytic performance of calcium titanate prepared via the direct reduction of VTCE

Under the conditions of a $CaCO_3$ dosage of 18wt% and a reduction temperature of 1400°C, the formation of calcium titanate in the reduction products was improved when the reduction time was increased from 150 to 210min. To determine whether the calcium titanate prepared in the reduction of VTCE could be used as a photocatalyst, the photocatalytic properties of the calcium titanate prepared via this method were systematically investigated.

3.2.1. Separation of calcium titanate and metallic iron

Before the effect of the reduction time on the calcium titanate photocatalysis was investigated, the reduction products at different times were firstly separated via magnetic separation to obtain calcium titanate and reduced iron. The results of reduced iron index were shown in Fig. 6. The conditions of the grinding magnetic separation were as follows: the primary grinding time was 10min, the first magnetic field intensity was 279kA/m, the secondary grinding time was 10min, and the secondary magnetic field intensity was 127kA/m.

As shown in Figs. 6(a) and 6(b), with an increase in the reduction time, the Fe grade in the reduced iron first increased and then decreased, the Fe recovery rate in the reduced iron gradually decreased. Meanwhile, the TiO_2 content in the reduced iron first decreased and then increased. When the reduction time was 150min, the Fe grade, Fe recovery rate and TiO_2 content in the reduced iron was 89.72wt%, 94.00wt% and 1.57wt%, respectively. When the reduction time was 180min, they were 90.95wt%, 92.21wt% and 0.95wt%, respectively. When the reduction time was 210min, they were 87.13wt%,

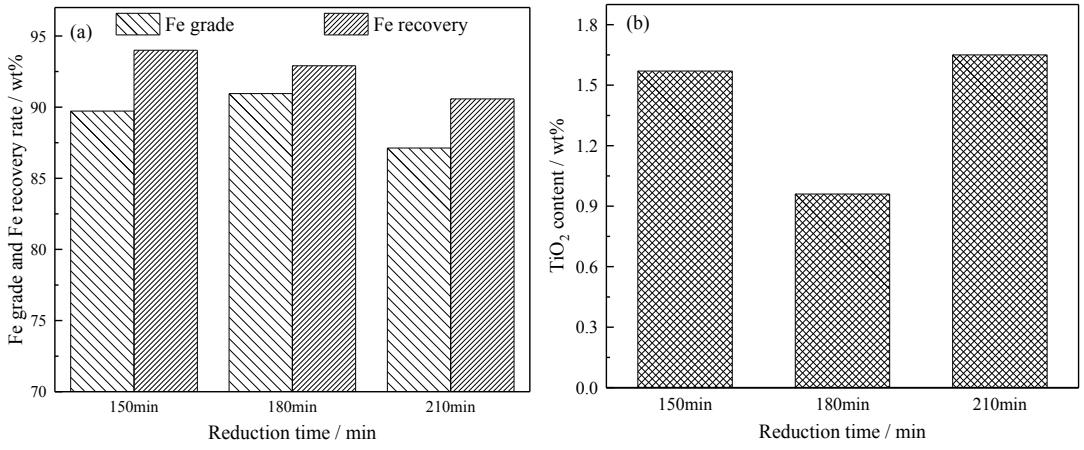

(a)-Fe grade and recovery rate in the reduced iron (b)-TiO_2 content in the reduced iron

Fig. 6. Reduced iron index at different reduction time

90.58wt% and 1.65wt%, respectively. Clearly, the reduced iron obtained at 180min was a qualified iron product as the Fe grade and recovery rate in the reduced iron were higher than 90wt%, and the TiO_2 content was less than 1wt%.

According to the above analysis results, the optimum reduction time was 180min under the conditions of $CaCO_3$ dosage of 18wt%, reduction temperature of 1400℃ and lignite dosage of 70wt%, where the reduced iron with Fe grade of 90.95wt% and Fe recovery of 92.21wt% can be obtained by grinding-magnetic separation. So, the XRD quantitative analysis was only carried out on calcium titanate obtained under the reduction time of 180min, the results are shown in Table 2.

Table 2. XRD quantitative analysis of calcium titanate

Mineral name	calcium titanate	diopside	Spinel	Forsterite	iron
Content / wt%	68	15	6	7	4

It can be found from Table 2 that the content of calcium titanate is the highest at 68wt%, followed by diopside at 15wt%. The content of spinel and forsterite is 6wt% and 7wt% respectively, and the lowest content of iron is 4wt%, which indicates that calcium titanate is the main phase composition in the non-magnetic product after magnetic separation, but its purity is relatively lower, so further optimizing the reduction conditions and conducting acid leaching test, etc. will be the focus in the future study.

3.2.2. Effect of reduction time on photocatalytic property of calcium titanate

According to the foregoing analysis results, a qualified iron product with an Fe grade of 94.84wt%, Fe recovery rate of 89.98wt% and TiO_2 content of 0.82wt% was obtained through the grinding-magnetic separation in the reduction of VTCE with the addition of $CaCO_3$. To further find out whether the calcium titanate prepared during the direct reduction of VTCE could be used as a photocatalyst, the photocatalytic properties of this calcium titanate prepared at different reduction times were investigated. The results were shown in Fig. 7.

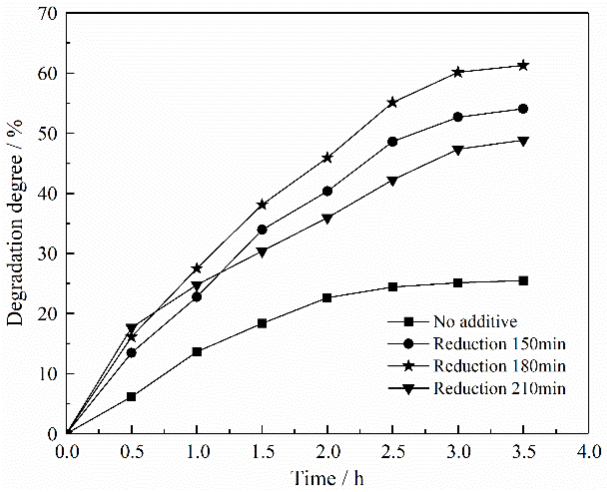

Fig. 7. Effect of reduction time on the degradation degree of methylene blue with or without calcium titanate

As shown in Fig. 7, the calcium titanate prepared in the reduction of VTCE with the addition of $CaCO_3$ had the ability to degrade methylene blue. Without the addition of calcium titanate, the degradation degree of methylene blue increased gradually with the extension of the UV irradiation time, approaching an equilibrium after 3h of reaction and reaching to 25.13%. Clearly, the degradation of methylene blue was poor without the photocatalyst under the UV irradiation conditions. After the addition of the calcium titanate, the degradation degree of methylene blue was significantly increased, confirming that the calcium titanate prepared during the direct reduction of VTCE had the ability to degrade methylene blue under the UV irradiation, while its photocatalytic activity exhibited a significant dependence on the reduction time changes. When the reduction time was 150min, the

photocatalytic degradation degree of methylene blue by calcium titanate increased gradually with the extension of UV irradiation time, approaching equilibrium after 3h of reaction and reaching to 52.68%. When the reduction time was extended 180min and 210min, the photocatalytic degradation degree of methylene blue by calcium titanate was 60.14% and 47.34%, respectively. The photocatalytic activity of calcium titanate obtained after 180min of reduction was significantly better than that of the calcium titanate obtained after 150 min and 210 min of reduction. Thus, considering of the effect of the reduction time on the reduced iron index and calcium titanate photocatalytic performance, the optimum reduction time was 180min.

It can be seen from the foregoing analyses that calcium titanate prepared in the direct reduction of VTCE shows better photocatalytic performance. However, according to the relevant literatures (Han, 2010; Wang et al., 2018), it can be known that the photocatalytic degradation rate of methylene blue by pure calcium titanate synthesized by solid-phase reaction can reach more than 75% under similar conditions. Although the photocatalytic degradation rate of methylene blue by calcium titanate obtained by the direct reduction method is relatively lower, the calcium titanate is obtained simultaneously in the reduction of iron in VTCE, which is conducive to the comprehensive recovery of titanium and iron resources in VTCE. In addition, in order to improve the photocatalytic activity of calcium titanate prepared by direct reduction method, optimizing reduction conditions and separation methods, and changing photocatalytic conditions (including calcium titanate dosage, methylene blue concentration, and pH of reaction solution) will be the focus in the future research.

3.2.3. Effect of reduction time on the photocatalytic reaction kinetics of calcium titanate

The degradation kinetics of the photocatalytic reaction are usually described by the Langmuir Hinshelwood model. According to the kinetic mechanism of Langmuir Hinshelwood, the reaction solution conformed to the first-order reaction kinetics. Assumed that the photocatalytic degradation of methylene blue by calcium titanate conformed to the first-order reaction kinetics, the rate equation was expressed by Eq. (3), and the Eq. (4) was obtained after integration.

$$\frac{dc_t}{dt} = -kc_t \tag{3}$$

$$ln\frac{c_t}{c_0} = -kt \tag{4}$$

where k was the first-order reaction rate constant, c_0 was the methylene blue concentration after reaching adsorption equilibrium, which as the initial concentration of photocatalytic reaction; c_t was the methylene blue concentration at time t. The photocatalytic degradation degree of methylene blue at different reduction time was converted according to equation (3), and the kinetic characteristics of photocatalytic degradation of methylene blue by calcium titanate at different reduction time were studied by linear fitting with $ln\ (c_t/c_0)$ as the ordinate and time as the abscissa.

As shown in Fig. 8, the straight line fitted under different reduction time conditions indicated a linear relationship. The correlation coefficient R_2 indicated that the fitting curves under the conditions of 150

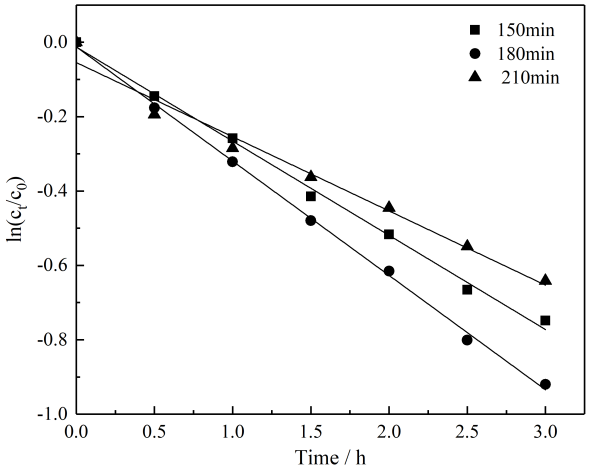

Fig. 8. Effect of reduction time on the photocatalytic degradation of methylene blue by calcium titanate

Table 3. Kinetic fitting equations and related parameters of photocatalytic degradation reaction at different reduction time

Time / h	Dynamic equation	k/hr	R^2	$T_{0.5}/h$
150min	$ln\ (c_t/c_0)$ =-0.2532t–0.0127	0.2532	0.9962	2.7370
180min	$ln\ (c_t/c_0)$ =-0.3073t–0.0123	0.3073	0.9984	2.2551
210min	$ln\ (c_t/c_0)$ =-0.1995t–0.0545	0.1995	0.9796	3.4736

min, 180min and 210min exhibited better correlation, indicating that the photocatalytic degradation of methylene blue by calcium titanate at different reduction times conformed to the first-order reaction kinetics model. It can be seen from Table 3 that with an increase in the reduction time, the photocatalytic degradation rate of methylene blue by calcium titanate first increased and then decreased, and the optimum effect was obtained when the reduction time was 180min.The results of SEM-EDS and grinding-magnetic separation revealed that at reduction times of 150min and 210min, the calcium titanate particles were too fine to be well separated with metallic iron, which reduced the contact area between the calcium titanate particles and the methylene blue, and reduced the adsorption capacity of the calcium titanate on methylene blue. Additionally, the numbers of electron hole pairs on the surfaces of calcium titanate particles and hydroxyl radicals with strong oxidation were reduced, which may be the reason for the poor degradation of methylene blue by calcium titanate under this condition. The mechanism of the photocatalytic degradation of methylene blue by calcium titanate prepared via the direct reduction method will be further investigated in future research.

4. Conclusions

Effect of direct reduction time of vanadium titanomagnetite concentrate on the preparation and photocatalytic performance of calcium titanate was investigated, and the conclusions were shown as follows.

1) The extension of the reduction time can not only promote the formation of calcium titanate, but also facilitate the reduction of iron minerals in the reduction products. The optimum reduction time was 180min under the conditions of $CaCO_3$ dosage of 18wt%, reduction temperature of 1400℃ and lignite dosage of 70wt%, where the metallization rate of iron reached 96.20wt%.

2) Under the conditions of the first magnetic field intensity of 279kA/m, the secondary magnetic field intensity of 127kA/m, the reduced iron (Fe grade of 90.95wt%, Fe recovery of 92.21wt%) and calcium titanate can be obtained by grinding-magnetic separation.

3) Without calcium titanate, the degradation effect of methylene blue was poor, approaching equilibrium after 3h and reaching to 25.13%. After the addition of calcium titanate obtained with 180min of reduction, the degradation degree increased to 60.14% under the same conditions, indicating that the calcium titanate prepared in the direct reduction of VTCE can be used as a photocatalyst.

4) Langmuir-Hinshelwood fitting results indicated that the methylene blue degradation by the calcium titanate basically conformed to the first-order reaction kinetics, and the photocatalytic degradation rate of methylene blue is highest when the reduction time is 180 min.

Acknowledgments

This research work was financially supported the National Natural Science Foundation of China (Grant No. 51674018).

References

ANI, I., AKPAN, J. U. G., OLUTOYE, M. A., HAMEED, B. H., 2018. *Photocatalytic degradation of pollutants in petroleum refinery wastewater by TiO_2-and ZnO-based photocatalysts: Recent development*. Journal of cleaner production. 205, 930-954.

ALSAYEGH, S., JOHNSON, R. O., BURKHARD, J., WESSLING, M., 2019. *Methanol production via direct carbon dioxide hydrogenation using hydrogen from photocatalytic water splitting: Process development and techno-economic analysis*. Journal of cleaner production. 208, 1446-1458.

CHEN, C., SUN, T. C., WANG, X. P., HU, T. Y., 2017. *Effects of MgO on the reduction of vanadium titanomagnetite concentrates with char*. Journal of Minerals, Metals & Materials Society. 69(10), 1759-1766.

CHEN, S. Y. CHU. M. S., 2014. *Metalizing reduction and magnetic separation of vanadium titano-magnetite based on hot briquetting*. International Journal of Minerals Metallurgy Material. 21(3), 225-233.

DENG, B. P., SI, X., BAUMAN, L. J., RAO, M. J., PENG, Z. W., JIANG, T., LI, G. H., ZHAO, B. X., 2020. *Photocatalytic activity of $CaTiO_3$ derived from roasting process of bauxite residue.* Journal of cleaner production. 244, 1-10.

HAN CHONG, 2010. *Solid state synthesis and the photocatalytic performanceof $CaTiO_3$*. Northeast University. (In Chinese)

HOLLIDAY, S., STANISHEVSKY, A., 2004. *Crystallization of $CaTiO_3$ by sol-gel synthesis and rapid thermal processing.* Surface and Coatings Technology. 188-189, 741-744.

IMTIAZ, M., RIZWAN, M., XIONG, S. L., LI, H. L., ASHRAF, M., SHAHZAD, S., 2015. *Vanadium, recent advancements and research prospects: a review.* Environment International. 80, 79-88.

LEI, X., XU. B., YANG, B., XU, B. B., GUO, X. T., 2017. *A novel method of synthesis and microstructural investigation of calcium titanate powders*, Journal of Alloys and Compounds. 690, 916-922.

LI, J., ZHANG, Y. C., WANG, T. X., ZHANG, M., 2011. *Low temperature synthesis and optical properties of $CaTiO_3$ nanoparticles from $Ca(NO_3)_2 \cdot 4H_2O$ and TiO_2 nanocrystals.* Materials Letters. 65, 1556-1558.

LI, X. H., KOU, J., SUN, T. C., WU, S. C., ZHAO, Y. Q., 2019. *Effects of temperature on Fe and Ti in carbothermic reduction of vanadium titanomagnetite with adding MgO*. Physicochemical Problems of Mineral Processing. 55(4), 917-927.

LI, X. H., KOU, J., SUN, T. C., WU, S. C., ZHAO, Y. Q., 2020a. *Effects of calcium compounds on the carbothermic reduction of vanadium titanomagnetite concentrate.* International Journal of Minerals Metallurgy Material. 27(3), 301-309.

LI, X. H., KOU, J., SUN, T. C., WU, S. C., ZHAO, Y. Q., 2020b. *Formation of calcium titanate in the carbothermic reduction of vanadium titanomagnetite concentrate by adding $CaCO_3$.* International Journal of Minerals Metallurgy Material. 27(6), 745-753.

LI, Z., WANG, Z., LI, G., 2016. *Preparation of nano-titanium dioxide from ilmenite using sulfuric acid-decomposition by liquid phase method*. Powder Technology. 287, 256-263.

MAO, H. X., ZHANG, R. D., LV, X. L., BAI, C. G., HUANG, X. B., 2013. *Effect of surface properties of iron ores on their granulation behavior*. ISIJ International. 53(9), 19-23.

MAN, Y., FENG, J. X., LI, F. J., GE, Q. Y., CHEN, M., ZHOU, J. Z., 2014. *Influence of temperature and time on reduction behavior in iron ore-coal composite pellets.* Powder Technology. 256, 361-366.

PAN, F., DU. Z., ZHANG, M. J., SUN, H. Y., 2017. *Relationship between the phases, structure, MgO migration and the reduction performance of the pre-oxidized vanadium-titanium magnetite ore in a fluidized bed.* ISIJ International 57(3), 413-423.

PAN, P. W., CHEN, Y. W., 2007. *Photocatalytic reduction of carbon dioxide on $NiO/InTaO_4$ under visible light irradiation.* Catalysis Communications. 8, 1546-1549.

PALANIANDY, S., JAMIL, N. H., 2009. *Influence of milling conditions on the mechanochemical synthesis of $CaTiO_3$ nanoparticles.* Journal of Alloys and Compounds. 476(1-2), 1-902.

SINGH, P., BORTHAKUR. A., 2018. *A review on biodegradation and photocatalytic degradation of organic pollutants: A bibliometric and comparative analysis*. Journal of cleaner production. 196, 1669-1680.

SREETHAWONG, T., LAEHSALEE, S., CHAVADEJ, S., 2009. *Use of Pt/N doped mesoporous assembled nanocrystalline TiO_2 for photocatalytic H_2 production under visible light irradiation.* Catalysis Communications. 10, 538-543.

SUN, Y. ZHENG, H. Y., DONG, Y., JIANG, X., SHEN, Y. S., SHEN, F. M., 2015. *Melting and separation behavior of slag and metal phases in metallized pellets obtained from the direct-reduction process of vanadium-bearing titanomagnetite*. International Journal of Mineral Processing. 142, 119-124.

WANG S S, ZHOU Y X, HAN S W, NONG, Y., 2018. *Carboxymethyl cellulose stabilized zno/biochar nanocomposites: enhanced adsorption and inhibited photocatalytic degradation of methylene blue.* Chemosphere Environmental Toxicology & Risk Assessment. 197, 20-25.

XIAO, Q., ZHANG, J., XIAO, C., 2008. *Photocatalytic degradation of methylene blue over Co3O4/Bi2WO6 composite under visible light irradiation*. Catalysis Communications. 9, 1247-1253.

YANG, F. L., HLAVACEK, V., 2000. *Effective extraction of titanium from rutile by a low-temperature chloride process.* Aiche Journal. 46(2), 355-360.

YI, L. Y., HUANG, Z. C., JIANG, T., 2013. *Sticking of iron ore pellets during reduction with hydrogen and carbon monoxide mixtures: behavior and mechanism*. Powder Technology. 235, 1001-1007.

YU, W. SUN, T. C., CUI, Q., XU, C. Y., KOU, J., 2015. *Effect of coal type on the reduction and magnetic separation of a high-phosphorus oolitic hematite ore*. ISIJ International. 55(3), 536-554.

YUE, X., LI, Q. Q., LI, B., ZHAO, L., WU, Y., YANG, T. Y., LIU, K., ZHANG, J. B., ZHU, N., 2019. *Novel CS_2 storage materials from ion-like liquids for one-step synthesis of active nano-metal sulfides in the photocatalytic reduction of CO_2.* Journal of cleaner production. 237, 1-9.

ZHANG, H. J., CHEN, G. G., LI, Y. X., TENG, Y. J., 2012. *Electronic structure and photocatalytic properties of copperdoped $CaTiO_3$.* Journal of Alloys and Compounds. 516, 91-95.

ZHAO, H. Y., DUAN, Y. W., SUN, X., 2013. *Synthesis and characterization of $CaTiO_3$ particles with controlled shape and size*. New Journal of Chemistry, 37(4), 986-991.

ZHANG, J., ZHANG, H. W., XUE, Z. L., 2017. *Oxidation Kinetics of Vanadium Slag Roasting in the Presence of Calcium Oxide,* Mineral Processing and Extractive Metallurgy Review. 38, 1-9.

ZHANG, Y. B., LU, M. M., ZHOU, Y. L., SU, Z. J., LIU, B. B., LI, G. H., JIANG, T. 2018. *Interfacial interaction between humic acid and vanadium, titanium-bearing magnetite (VTM) particles.* Mineral Processing and Extractive Metallurgy Review. 2, 1–10.

ZHAO, Y. Q., SUN, T. C., ZHAO, H. Y., CHEN, C., WANG. X. P., 2019. *Effect of reductant type on the embedding direct reduction of beach titanomagnetite concentrate*. International Journal of Minerals Metallurgy Material. 26(2), 152-159.